Contribution from the Institute of Inorganic Chemistry, University of Karlsruhe, Karlsruhe, West Germany, and Rockwell International, Rocky Flats Plant Building 779, Golden, Colorado 80401

Compositions and Crystal Structures of the Intermediate Phases in the Samarium–Bromine System

H. BÄRNIGHAUSEN and JOHN M. HASCHKE*

Received April 6, 1977

As a recent investigation of the samarium–bromine system has shown three closely spaced discrete phases $SmBr_x$ exist along the 450 °C isothermal section between $SmBr_2$ and $SmBr_3$. The present investigation has confirmed their existence and has employed available Guinier powder diffraction patterns (Cu $K\alpha_1$ radiation) for their structural characterization. The crystallographically determined compositions are $x = 2.167$ for phase I, $x = 2.182$ for phase II, and $x = 2.200$ for phase III. The closely related structures of the intermediates are derived from the fluorite-type structure by accommodation of additional anions in superstructure arrangements with long periodicities and provide additional examples of the so-called vernier structures. Phase I (Sm_6Br_{13}) and phase III (Sm_5Br_{11}) are clearly isostructural with Yb_5ErCl_{13} and Dy_5Cl_{11}, which have previously been characterized by single-crystal methods. A plausible structure that satisfactorily reproduces the line positions and intensities of the powder pattern is proposed for phase II ($Sm_{11}Br_{24}$).

Introduction

The rather complex phase equilibria of the samarium–bromine system at the 450 °C section are described in a recent article in this journal.[1] X-ray diffraction data indicate the existence of three intermediate phases, $SmBr_x$, with compositions in the range $2.10 < x < 2.18$. The reported stoichiometries of these phases, $SmBr_{2.129}$ (phase I), $SmBr_{2.140}$ (phase II), and $SmBr_{2.172}$ (phase III), are based on the results of chemical analyses for metal and halide contents. However, the determination of these compositions was complicated by presence of SmOBr contamination which was found to be present at levels of 1–2 mass % in the analyzed samples.

Recent single-crystal x-ray diffraction studies have resulted in the definition of the crystal structures and compositions of the intermediate lanthanide chloride phases Dy_5Cl_{11}[2] and Yb_6Cl_{13}.[3] After examining the x-ray diffraction data reported for the intermediate samarium bromides,[1] H.B. observed that two of these phases (I and III) appeared to be isostructural with the dysprosium and ytterbium chlorides and suggested that the compositions and structures of the samarium phases could be unambiguously defined by detailed evaluation of the crystallographic data.

The present collaborative investigation was undertaken in an effort to correct the stoichiometries in the original report[1] and to obtain structural data for the intermediate samarium bromides. The close similarity of the diffraction patterns reported for phases II and III suggested that phase II might not be unique. Consequently, the data for this compound have been examined with extra care.

Experimental Section

The present investigation of the structures of the intermediate samarium bromide phases has been accomplished by reexamination of existing powder x-ray diffraction data. High-quality films[1] obtained with a Guinier–Hägg camera (114.6-mm diameter, Cu $K\alpha_1$ radiation, λ 1.540 562 Å) were employed for the expanded study of the composition range of interest. The present work has been limited to a critical examination of these data and especially to a precise remeasurement of three important films. All readings were made with a coincidence micrometer (Hartmann and Braun, Frankfurt am Main, Germany) to an accuracy of 10^{-2} mm. For $\theta > 14°$, the measured values were calibrated with the diffraction lines of Si ($a_0 = 5.430\,94$ Å)[4] which was employed as an internal standard. For reflections with lower diffraction angles, calibrations were referenced to the 001 reflection ($\theta = 5.585°$ for $c = 7.914$ (2) Å) of SmOBr[5] which was present as a trace contaminant in all samples.

Comparison of the diffraction data listed as supplementary material with those of Table II in the earlier report[1] shows good agreement for the more intense diffraction lines; however, a number of additional weak reflections have been measured for all three intermediate phases. Most of the new lines are only slightly above background levels. The earlier data for $SmBr_{2.129}$ include an extraneous line ($d_o = 2.929$ Å) that does not appear in the present listing for Sm_6Br_{13}. This line is assignable as a coincidence of the 122, 212, 231, and 321 reflections of the $SrBr_2$-type[6] $SmBr_2$ and has been deleted from the diffraction pattern for phase I.

Results obtained during the refinement of the crystallographic data for phase II indicated that the 111 line ($d_o = 3.136$ Å) of the Si standard was coincident with an important reflection. A Guinier pattern obtained for a silicon-free sample of phase II showed the presence of a readily discernible line ($d_o = 3.139$ Å) which is not included in the earlier listing of d values. In the present listing (supplementary material) this line is identified as the coincidence of the 0,26,0 and 2,15,0 reflections of $Sm_{11}Br_{24}$.

In order to maintain a tractable quantity of diffraction data, only reflections with θ values less than 21° are included in the supplementary listing. The readable regions of the individual Guinier films extend well beyond this limit; for phases I, II, and III, θ values have been measured to 38, 28, and 35°, respectively. Higher angle reflections are not discernible above the background.

Crystallographic data for the three intermediate phases are presented in Table I. The lattice parameters were refined with 30–40 coincidence-free reflections using the least-squares program GIVER.[7] All calculations described in this report were performed with the Univac 1108 computer facility at the University of Karlsruhe.

Interpretation of the Diffraction Data

The basic conclusions of the previous work on the phase equilibria of the samarium–bromine system have been verified by the reevaluation of the diffraction data. Three intermediate phases are found between the $SrBr_2$-type dibromide and the $PuBr_3$-type tribromide. All reflections of phases I and III, which coexist with the di- and tribromides, respectively, have been indexed using the method of de Wolff.[8] In both cases, monoclinic subcells with the similar lattice parameters (a, b', and c) listed in Table I were found. The similarities of the cells were, however, evident only after appropriate settings had been selected. For phase I, [001] (first setting) was chosen as the unique crystallographic direction, and a [010] (second setting) was selected for phase III. Definition of the subcells permitted the assignment of substantial fractions of the diffraction lines, which are marked with single asterisks in the diffraction data included as supplementary material.

Identification of the subcells was especially important in that similar subcells are observed for the fully determined structures of the lanthanide chlorides Yb_6Cl_{13}[3] and Dy_5Cl_{11}.[2] Closely related structures have been assumed to exist for the bromides. By employing a sixfold multiple of the subcell ($a \times 6b' \times c$) like that of Yb_6Cl_{13}, the remaining unassigned reflections of phase I have been indexed. In a similar way, all lines for phase III are assigned to a fivefold supercell ($a \times 5b' \times c$) like that of Dy_5Cl_{11}. Conclusive evidence for the existence of isomorphism between the bromides and the chlorides is found in the results of intensity calculations presented as supple-

* To whom correspondence should be addressed at Rockwell International.

0020-1669/78/1317-0018$01.00/0

Table I. Crystallographic Data of the Intermediate Samarium Bromides[a]

	Phase I	Phase II	Phase III
Chemical formula	Sm_6Br_{13}	$Sm_{11}Br_{24}$	Sm_5Br_{11}
Formula wt	1940.85	3571.55	1630.69
x = Br/Sm ratio	2.167	2.182	2.200
n = no. of subcells along b	6	11	5
Crystal system	Monoclinic	Monoclinic	Monoclinic
Unique axis	[001]	[010]	[010]
Space group	$I2/a$ (No. 15)[b]	$P2_1/n$ (No. 14)[b]	$P2_1/m$ (No. 11)
Lattice constants: a, Å	7.649 (2)	7.652 (2)	7.652 (2)
b, Å	44.44 (2)	81.62 (6)	37.21 (2)
$b' = b/n$, Å	7.407 (3)	7.420 (5)	7.442 (4)
c, Å	7.139 (2)	7.130 (3)	7.121 (2)
angle, deg	$\gamma = 91.30$ (5)	$\beta = 90.19$ (7)	$\beta = 90.26$ (5)
V = vol of unit cell, Å^3	2425.4 (1.4)	4453 (4)	2027.5 (1.3)
$V' = V/n$ = vol of subcell, Å^3	404.2 (2)	404.8 (5)	405.5 (3)
Z = formula units/unit cell	4	4	4
D_x = calcd density, g/cm^3	5.315 (3)	5.327 (5)	5.342 (4)

[a] Estimated errors in the last digit are given in parentheses. [b] Unconventional setting of the respective space group. $I2/a$: $(0, 0, 0; {}^1/_2, {}^1/_2, {}^1/_2) \pm (x, y, z; {}^1/_2 + x, y, {}^1/_2 - z)$. $P2_1/n$: $\pm(x, y, z; {}^1/_2 + x, {}^1/_2 - y, {}^1/_2 + z)$.

mentary material. Calculated intensities were obtained using the program POWD 5[9] in which the form factors for Sm and Br are included as sums of Gaussian functions. The atomic coordinates and temperature factors for phases I and III (Table II) are derived from the numerical values of Yb_5ErCl_{13}[3] and Dy_5Cl_{11}.[2] Comparison of the observed and calculated intensities shows excellent agreement for both bromides; however, these results do not constitute an independent structure determination. Projections of the Sm_6Br_{13} and Sm_5Br_{11} structures appear in the upper and lower diagrams of Figure 1.

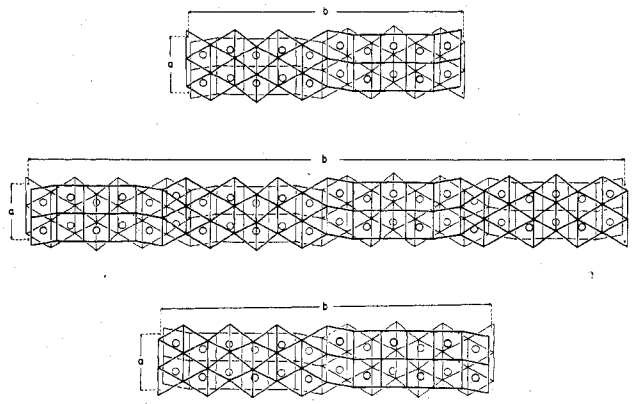

Figure 1. Projection of the vernier structures of Sm_5Br_{11}, $Sm_{11}Br_{24}$, and Sm_6Br_{13} on (001). (Samarian atoms at $z \approx 0$ and $\approx {}^1/_2$ are represented by light and bold circles, respectively. Bromine atoms have z values of approximately ${}^1/_4$ and ${}^3/_4$ and are located at the intersection points of the somewhat puckered nets.)

Since an isomorphous compound is not known for phase II, an equivalent crystallographic characterization is not possible. However, atomic coordinates are presented in Table III for a plausible structure which satisfactorily accounts for both the line positions and the intensities of the diffraction pattern of phase II. Comparison of the observed and calculated (POWD

Table II. Positional and Thermal Parameters of the Atoms for the Intermediate Samarium Bromides Sm_6Br_{13} (Phase I) and Sm_5Br_{11} (Phase III)[a]

Phase	Atom	x	y(I)[b]	y(III)	z	B, Å^2	Phase	Atom	x	y[c]	z	B, Å^2
I	Sm(1)	0.3291	0.45418		0.0247	1.08						
III	Sm(1)	0.3343	[0.45396]	0.44475	0.0232	1.43	III	Sm(4)	0.8351 (0.8343)	0.44492 (0.44475)	0.4711 (0.4768)	1.31
I	Sm(2)	0.7195	0.37051		0.0219	1.11						
III	Sm(2)	0.7404	[0.37132]	0.34558	0.0138	1.38	III	Sm(5)	0.2439 (0.2404)	0.34504 (0.34558)	0.4795 (0.4862)	1.42
I	Sm(3)	0.2990	0.28978		0.0184	1.09						
III	Sm(3)	0.3285	[0.29167]	0.25	0.0156	1.31	III	Sm(6)	0.8352 (0.8285)	0.25 (0.25)	0.4797 (0.4844)	1.07
I	Br(1)	0.606	0.4925		0.232	1.8						
III	Br(1)	0.610	[0.4926]	0.4911	0.232	2.1	III	Br(7)	0.104 (0.110)	0.4921 (0.4911)	0.273 (0.268)	2.5
I	Br(2)	0.646	0.4307		0.820	1.1						
III	Br(2)	0.658	[0.4310]	0.4172	0.811	2.2	III	Br(8)	0.150 (0.158)	0.4171 (0.4172)	0.674 (0.689)	1.9
I	Br(3)	0.511	0.4122		0.305	1.2						
III	Br(3)	0.535	[0.4125]	0.3950	0.304	2.1	III	Br(9)	0.025 (0.035)	0.3958 (0.3950)	0.194 (0.196)	1.7
I	Br(4)	0.364	0.3554		0.856	1.6						
III	Br(4)	0.373	[0.3590]	0.3308	0.873	1.9	III	Br(10)	−0.116 (−0.127)	0.3276 (0.3308)	0.631 (0.627)	2.4
I	Br(5)	0.511	0.3299		0.310	1.0						
III	Br(5)	0.545	[0.3303]	0.2963	0.314	1.5	III	Br(11)	0.031 (0.045)	0.2966 (0.2963)	0.189 (0.186)	1.4
I	Br(6)	0.666	0.2838		0.870	2.0						
III	Br(6)	0.689	[0.2917]	0.25	0.860	3.2	III	Br(12)	0.198 (0.189)	0.25 (0.25)	0.609 (0.640)	2.5
I	Br(7)	0.5	0.25		0.309	1.1						
III	Br(5′)[d]	0.545	[0.2531]	0.2037	0.314	1.5						

[a] Data for the isomorphic compounds Yb_5ErCl_{13}[3] and Dy_5Cl_{11}[2] have been adopted. The values for Sm_6Br_{13} (phase I) have been transferred to space group $I2/a$ (see text). [b] In order to demonstrate the close relationship between x, y, and z for phases I and III, the coordinates y(III) have been adjusted to the b axis of phase I by the transformation $[y(\text{I})] = {}^5/_6[y(\text{III}) + 0.1]$. [c] The small deviations from the higher symmetry space group *Pnma* are shown by the coordinates enclosed in parentheses. The values have been calculated from those for phase III on the left-hand side by employing the symmetry operation $({}^1/_2 + x, y(\text{III}), {}^1/_2 - z)$, i.e., the pseudo-glide plane. [d] Note that Br(5′) does not belong to the asymmetric unit of phase III; it has been obtained from Br(5) by the transformation $(x, {}^1/_2 - y, z)$ (mirror plane).

Table III. Proposed Structural Data for the Intermediate Samarium Bromide $Sm_{11}Br_{24}$ (Phase II)[a]

Atoms of the asymmetric unit compiled in parameter-related groups				Estd positional parameters[b]			
x, y, z	$^1/_2 + x, y, ^1/_2 - z$	x, y', z	$^1/_2 + x, y', ^1/_2 - z$	x	y	y'	z
Sm(1)	Sm(4)	Sm(7)	Sm(9)	0.333	0.4749	0.2978	0.026
Sm(2)	Sm(5)	Sm(8)	Sm(10)	0.740	0.4297	0.3430	0.016
Sm(3)	Sm(6)			0.330	0.3864		0.016
Sm(11)				0.180	0.25		0.5
Br(1)	Br(7)	Br(13)	Br(19)	0.608	0.496	0.277	0.232
Br(2)	Br(8)	Br(14)	Br(20)	0.649	0.462	0.310	0.822
Br(3)	Br(9)	Br(15)	Br(21)	0.529	0.453	0.320	0.308
Br(4)	Br(10)	Br(16)	Br(22)	0.379	0.422	0.350	0.869
Br(5)	Br(11)	Br(17)	Br(23)	0.539	0.408	0.365	0.316
Br(6)	Br(12)			0.683	0.386		0.872
Br(18)	Br(24)			0.420	0.269		0.768

[a] The nonconventional data format for atoms in the asymmetric unit is employed to clarify the structural proposal. With the exception of Sm(11), the coordinates of crystallographically independent atoms in each row have been derived from those of the appropriate atomic positions of the idealized Sm_5Br_{11} structure by use of the transformations appearing in the column headings. In this process, the x and z coordinates are adopted directly; the y coordinates are converted from the fivefold superstructure to the elevenfold superstructure by use of the formulas $y = {}^5/_{11}[y(\mathrm{III}) + 0.6]$ and $y' = {}^5/_{11}[1.1 - y(\mathrm{III})]$. [b] The thermal parameters employed for Sm and Br are 1.3 and 1.8 Å^2, respectively.

5)[9] values (supplementary material) shows good agreement for the proposed $Sm_{11}Br_{24}$ structure, which is based on the following experimental observations. (a) The strongest lines of the powder pattern are assignable to a monoclinic subcell with parameters very similar to those of phase III (cf. Table I). In this case, [010] (second setting) must be chosen as the unique direction. In the supplementary material, the subcell reflections of phase II are also marked with single asterisks. (b) By assuming an 11-fold supercell ($a \times 11b' \times c$), all the diffraction lines of phase II have been indexed. An especially convincing aspect of this subcell–supercell relationship is demonstrated by examining the relative line positions of the 0,14,0, 0,26,0, and 0,12,0 reflections and of the 0,13,1, 0,24,1, and 0,11,1 reflections for phases I, II, and III, respectively. For each of the phases, these reflections are displaced by approximately equal amounts from the adjacent subcell lines, and they have played a key role in identifying the superstructure. (c) A close correspondence is evident in the intensity distributions of the diffraction lines of phases II and III. Consequently, the structure of phase III has been employed as much as possible as a model for that of phase II.

Examination of a projection of the proposed structure for phase II in the middle of Figure 1 shows that its center section corresponds exactly to a unit cell of Sm_5Br_{11}. Both sides of this section are flanked by glide planes, n, which are so placed that repetition of the Sm_5Br_{11} cell under the symmetry operation leads directly to a supercell containing the desired 11-fold multiple of the subcell. Almost all of the atomic coordinates of atoms in the asymmetric unit of phase II (Table III) may be directly derived from the assumed coordinates of the Dy_5Cl_{11}-type Sm_5Br_{11} (Table II). The asymmetric unit must also contain a metal atom in addition to those of the Sm_5Br_{11} cells, but its positional coordinates are unknown. It is obvious that this atom, Sm(11) in Table III, must lie in the glide plane mentioned above and that its exact position must be consistent with the structural principles of the intermediate bromides. It should be noted that the x, y, and z coordinates of the asymmetric unit of phase II (Table III) have been derived from a somewhat idealized structural model of Sm_5Br_{11}. Like the isomorphous compound Dy_5Cl_{11}, Sm_5Br_{11} can be described in a very good approximation by the higher symmetry space group *Pnma*.[2] The atoms of the appropriate asymmetric unit have coordinates x, y, and z which are almost the same as those given for phase III on the left-hand side of Table II. Although the proposed structure for phase II is based on this rather crude model, its application in the derivation of atomic coordinates is justified.

In addition, the asymmetric unit of phase I is also closely related to the idealized structure of Sm_5B_{11}. This can be seen immediately by examination of Table II and Figure 1. For this demonstration, however, it was necessary to depart from the conventional crystallographic description of Sm_6Br_{13} (Yb_5ErCl_{13} structure type[3]). By use of the relationships $a = -c_0$, $b = a_0 + c_0$, and $c = -b_0$, the structure of Yb_5ErCl_{13} has been transformed from the standard literature setting a_0, b_0, c_0 (space group $C12/c1$) to an equivalent form (space group $I112/a$). The origin has also been shifted and a different asymmetric unit has been defined by an alternate selection of atoms.

Discussion

The present investigation has confirmed the existence of three intermediate phases between $SmBr_2$ and $SmBr_3$ and has permitted a precise definition of their Br:Sm ratios, x, from their x-ray diffraction data. In comparison to the crystallographically determined compositions ($SmBr_{2.167}$, $SmBr_{2.182}$, and $SmBr_{2.200}$), the previously reported values[1] ($SmBr_{2.129}$, $SmBr_{2.140}$, and $SmBr_{2.172}$) are consistently low by 0.03–0.04 in x, and a systematic error in the analytical method is suggested. Although the analytical procedure included a correction for oxide contamination, the SmOBr contents could easily be twice the gravimetrically determined 1–2 mass % levels.

An additional comment related to the stoichiometry of the bromides concerns the first observation of an intermediate phase in the samarium–bromine system. Jantsch and Skalla[10] reported that $SmBr_3$ decomposes at temperatures above 700 °C to form a residue with the composition $SmBr_{2.19}$. Within the limits of analytical uncertainty, this product is Sm_5Br_{11}, and it is now clear that its formation corresponds to the first step in the reduction of the tribromide.

Until recently, definitive structural results have been unavailable for either the intermediate samarium bromides or other intermediate phases in the rare earth–halide systems, Ln + X. Only speculative structural models[1,11,12] based on the principle of coherent intergrowth of regions of LnX_2 and LnX_3 with their known structure types have been available. Two recent independent structure determinations[2,3] employing three-dimensional data demonstrate that the models are all incorrect. Recent results[2] show that the structures are actually based on a fluorite-related structure in which the cationic sublattice is retained and the anions are partially rearranged to accommodate additional anions. Half of the characteristic square nets of the anionic sublattice are retained, but the other

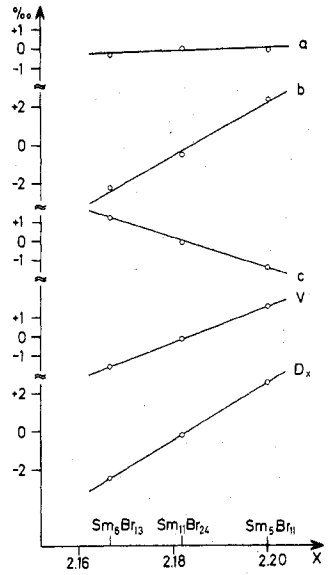

Figure 2. Relative changes in the crystallographic data for the subcells across the series of intermediate samarium bromides (cf. Table I).

half are converted to a hexagonal closest packed array. The space filling within the rearranged part of the structure is improved by 7.8%, and additional anions can therefore be incorporated.

The structures of the intermediate samarium bromides are included within the general concept of so-called "vernier structures", a designation that has recently evolved from observations with other materials.[12] The projections in Figure 1 clearly demonstrate how the overlapping anionic nets with the two different types of packing create the visual impression of a vernier scale. However, with the structures of the intermediate rare earth halides, the vernier picture is an idealization. A careful examination of the projections in Figure 1 shows that a small "imperfection" must be accommodated by the structures. In each case, the length of a section of square anion net along (010) does not exactly match that of the corresponding hexagonal net. The sections of hexagonal net contain an additional row of anions and are slightly longer than those of the square net. In each of the structures, this mismatch is accommodated by a periodic alternation of the square and hexagonal nets within each anionic layer. It should be mentioned that in the structures of other vernier phases ($Zr_{54}N_{49}F_{69}$[13] and $Y_7O_6F_9$[14]) the anionic arrays are precisely coherent and such alternations within the unit cell are unobserved. The specific crystal–chemical parameters which determine whether the anion nets are alternating or continuous have not been identified.

As is frequently the case for systems with a sequence of closely spaced discrete phases, the compositions of the intermediate samarium bromides are described by an homologous series. Phases III, II, and I correspond, respectively, to the n = 10, 11, and 12 members of a series with the general formula M_nX_{2n+2}. The experimental results verify that the samarium–bromine system is limited to these three members along the 450 °C isothermal section, and, consequently, four two-phase regions are observed between $SmBr_2$ and $SmBr_3$. The vernier phases observed in other rare earth–halide systems are also assignable as members of M_nX_{2n+2} series for the same limited ranges of n.[2] It appears that substantially more vernier phases of the homologous series are present in the unusually complex thulium–chlorine system investigated by Caro and Corbett,[15] and the structural characterization of the intermediate thulium chlorides is recognized as an especially important area for additional work.

Although the general structural characteristics of the intermediate samarium bromides have been defined, some of the finer points also merit discussion. A good overview is given by the modified Vegard-type graph in Figure 2. The relative variations of the crystallographic parameters in Table I are shown as a function of composition, x. It is evident that the magnitudes of these changes are only slightly greater than their experimental uncertainties. The relative values are, however, believed to be valid because they are based on a consistent set of film measurements that are at least a factor of 2 more precise than the error limits given in Table I.

An examination of the projections in Figure 1 shows that the a dimensions of the three intermediate phases equal the combined diameters of two bromide ions, and as expected, the observed a parameters are essentially independent of composition. The distance (7.68 Å) calculated by using 1.92 Å as the effective radius of a Br^- with an average coordination number of 3.5 is in close agreement with the experimental parameters (7.649–7.652 Å). As x increases from Sm_6Br_{13} to Sm_5Br_{11}, additional anions must be accommodated by the CaF_2-related substructure. From knowledge of the vernier principle, it is clear that these anions are added along the b axis and result in a regular elongation in the [010] direction. It is especially interesting that both the subcell volume and the density increase with increasing bromide content. Although a decrease in density might actually be expected, its relative increase is even greater than that of the volume. One must conclude that the packing becomes increasingly more efficient within the series between phases I and III. Since a continued increase in packing efficiency is not possible for the vernier-type structures, the observed termination of the M_nX_{2n+2} series at Sm_5Br_{11} can in principle be understood.

The present results have been obtained by adopting the atomic positions of isomorphous phases, and it is not possible to present further structural details for the intermediate samarium bromides. The ordering of divalent and trivalent cations on crystallographically inequivalent sites is of special crystal–chemical interest. The problem has been substantially clarified for Dy_5Cl_{11},[2] but this aspect of the bromide structures remains undefined.

Acknowledgment. The support of J.M.H. by the Department of Chemistry at the University of Michigan during the experimental aspects of this work is gratefully acknowledged.

Registry No. Sm_6Br_{13}, 57559-83-8; $Sm_{11}Br_{24}$, 60616-37-7; Sm_5Br_{11}, 60616-36-6.

Supplementary Material Available: A listing of observed and calculated interplanar distances and diffraction intensities for the intermediate samarium bromides (4 pages). Ordering information is given on any current masthead page.

References and Notes

(1) J. M. Haschke, *Inorg. Chem.*, **15**, 298 (1976).
(2) H. Bärnighausen, *Proc. Rare Earth Res. Conf., 12th*, **1**, 404 (1976).
(3) H. Lüke and H. A. Eick, *Proc. Rare Earth Res. Conf., 12th*, **1**, 424 (1976).
(4) T. Hom, W. Kiszenick, and B. Post, *J. Appl. Crystallogr.*, **8**, 457 (1975).
(5) H. Bärnighausen, G. Brauer, and N. Schultz, *Z. Anorg. Allg. Chem.*, **338**, 250 (1965).
(6) J. G. Smeggil and H. A. Eick, *Inorg. Chem.*, **10**, 1458 (1971).
(7) K. Krogmann, "An ALGOL Least-Squares Program for Refinement of Lattice Dimensions", University of Karlsruhe, 1971.
(8) P. M. de Wolff, *Acta Crystallogr.*, **10**, 590 (1957).
(9) C. M. Clark, D. K. Smith, and G. G. Johnson, "A FORTRAN IV Program for Calculating X-Ray Powder Diffraction Patterns", Version 5, The Pennsylvania State University, 1973.
(10) G. Jantsch and N. Skalla, *Z. Anorg. Allg. Chem.*, **193**, 391 (1930); see p 400.
(11) P. E. Caro, *Natl. Bur. Stand. (U.S.), Spec. Publ.*, **No. 364**, 367 (1972).
(12) B. G. Hyde, A. N. Bagshaw, S. Andersson, and M. O'Keeffe, *Annu. Rev. Mater. Sci.*, **4**, 43 (1974); see pp 56 and 82.
(13) W. Jung and R. Juza, *Z. Anorg. Allg. Chem.*, **399**, 129 (1973).
(14) D. J. M. Bevan and A. W. Mann, *Acta Crystallogr., Sect. B*, **31**, 1406 (1975).
(15) P. E. Caro and J. D. Corbett, *J. Less-Common Met.*, **18**, 1 (1969).